Journal of Materials Chemistry C

Accepted Manuscript

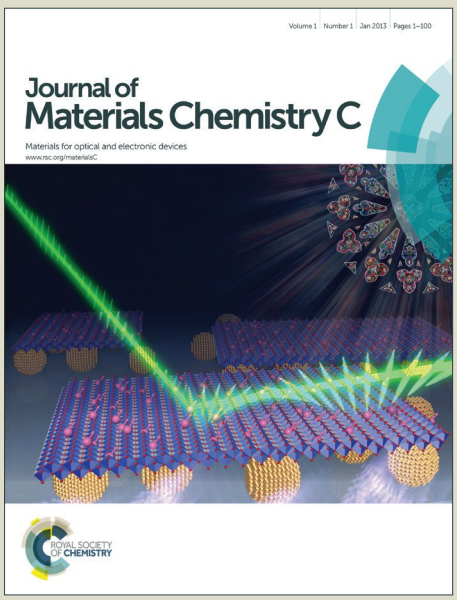

ROYAL SOCIETY OF CHEMISTRY

www.rsc.org/materialsC

Cite this: DOI: 10.1039/c0xx00000x

www.rsc.org/xxxxxx

ARTICLE TYPE

Hole Mobility of 3.56 $cm^2V^{-1}s^{-1}$ Accomplished Using More Extended Dithienothiophene with Furan Flanked Diketopyrrolopyrrole Polymer

Prashant Sonar,[a, b*] Jingjing Chang,[a, c] Zugui Shi,[a] Eliot Gann,[d, e] Jun Li,[a] Jishan Wu,[a, c] Christopher R McNeill [e]

Received (in XXX, XXX) XthXXXXXXXXX 20XX, Accepted Xth XXXXXXXXX 20XX
DOI: 10.1039/b000000x

Highly extended dithienothiophene comonomoer building block was used in combination with highly fused aromatic furan substituted diketopyrrolopyrrole for the synthesis of novel donor-acceptor alternating copolymer **PDPPF-DTT**. Upon testing **PDPPF-DTT** as a channel semiconductor in top contact bottom gate organic field effect transistors (OFETs), it exhibits p-channel behaviour. The highest hole mobility of 3.56 cm^2/vs was reported for **PDPPF-DTT**. To our knowledge, this is the highest mobility reported so far for the furan flanked diketopyrrolopyrrole class of copolymers using conventional device geometry with straightforward processing.

Introduction

Since last decade, there are several reports on high performance polymeric semiconductors for the *p*-channel and *n*-channel organic field effect transistors (OFETs).[1-4] Since last few years, a significant progress has been made towards the development of a solution processable high mobility organic semiconducting polymeric materials. [1-4] Nowadays achieving mobility higher than 0.1 cm^2/Vs in organic field effect transistors (OFETs) devices become a very common trend in various worldwide labs due to exploration of new building blocks and their effective utilization for designing a new polymeric organic semiconductors.[5-7, 2] Such a high performance materials are absolutely important for making flexible printed organic electronic devices for various applications ranging from complementary circuits, driver for active matrix display, sensors, and active donor materials for organic photovoltaics.[8-11] Among reported various polymeric structures, donor-acceptor (D-A) based alternating copolymers becomes one of the most successful design regulation to achieve high performance in both OFETs and organic photovoltaics.[12-18] D-A copolymers improves the intramolecular interaction due to the orbital overlap of highest occupied molecular orbital (HOMO) of donor and the lowest unoccupied molecular orbital (LUMO) of acceptor which causes widening of UV-vis-NIR absorption and reduction in band gap. Low energy charge transfer transitions and the crystallinity can be enhanced through partial polarity on the D-A moieities.[1,17,18] On the basis of ionization potential of donor and the electron affinity of acceptor incorporated in the conjugated backbone, the copolymers can be classified into strong donor-strong acceptor, strong donor-weak acceptor, weak donor-strong acceptor and weak donor-weak acceptor respectively.[19-22] In addition to that, the planarity of the fused aromatic building blocks in the conjugated backbone, inter-chain interaction, donor-acceptor partially polarity determines the π-π stacking and interlayer d-spacing of the polymeric chains.[23, 17, 18] There are numerous donor-acceptor based copolymers have been reported in the literature for high performing OFET devices but among them, most of the reported highest mobility copolymers are either made up of diketopyrrolopyrrole (DPP)[1,4,13], isoindigo (IS)[24] or other fused aromatic conjugated building blocks in the main backbone.[25,26, 2] These all fused rings have common feature of lactam units which assist for better orbital overlapping, enhancing intermolecular interaction and inducing solution processibility due to long branched alkyl chain substitution on the nitrogen atom.

Recently, DPP based polymeric materials have attracted significant attention in the organic electronic community due to its low cost, easy synthesis, wide scope of structural variation with respect to selection of heterocyclic moiety at 2, 5-positions. π-π Intermolecular interactions, and optical properties of such materials can be easily tuned by using various conjugated blocks adjacent to the DPP.[1, 27] The planarity in such heterocyclic flanked DPP structures can be induced due to the substitution of various heteroatoms such as sulfur, oxygen, selenium and nitrogen on thiophene/furan/selenophene/pyridine and their interaction with oxygen substituted on carbonyl group. Such a intramolecular interaction can significantly enhance the π-π interaction.[1,28] In the literature, most of the materials are based on the thiophene flanked DPP (DPPT) but there are very few reports on furan flanked DPP (DPPF) materials. [29-35] Furan is also one of the most important biological degradable green conjugated building blocks and has not explored in detail yet for synthesizing organic semiconductors. Furan can be successfully and effectively utilized in combination with DPP for designing new high performance solution processable organic semiconductors. Since last few years, our group has been developing furan flanked DPP based conjugated polymers for elevating its performance in OFET devices via rational design principle.[36, 37] On the other hand, linearly fused oligothiophene-based compounds derived from dithieno [3, 2-b: 2', 3'-d] thiophene (DTT) have been successfully used in a variety of organic optoelectronic devices,

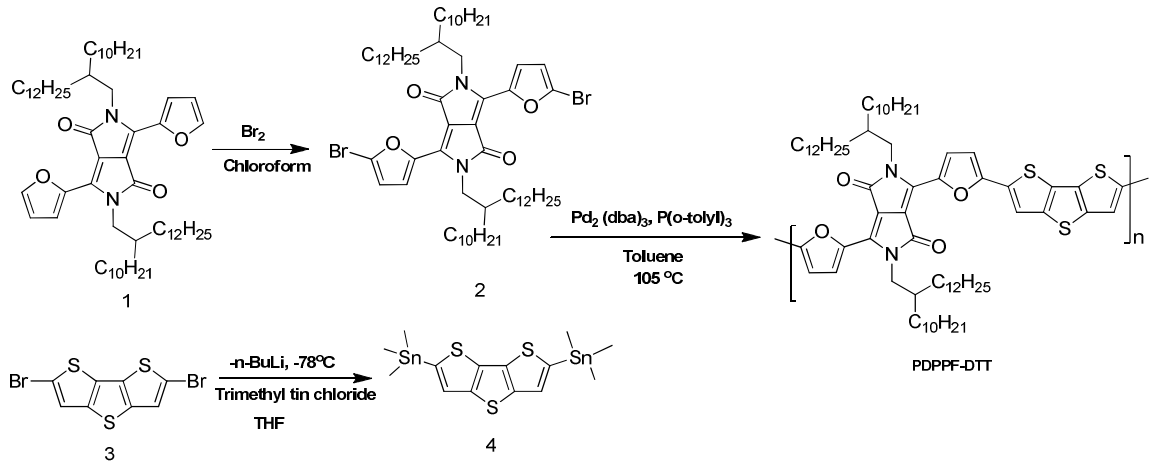

Scheme 1 Synthesis of **PDPPF-DTT** via Stille coupling polymerization.

because the DTT unit has relatively high hole mobility due to the fused thiophene core.[38-40] A fused thiophene motifs such as dithienothiophene are well known for their strong intermolecular S..S interactions and structural planarity.[41-43] The sulfur rich electron donating DTT unit exhibits structural rigidity in conjugated backbone arising from its fused chemical structure, and therefore DTT building blocks in combination with furan flanked DPP may achieve higher performance in OFET devices.

In this work, we report the design and synthesis of a solution-processable *p*-channel polymer semiconductor **PDPPF-DTT** (Scheme 1), which showed the highest hole mobility of 3.56 cm^2/Vs in top contact bottom gate OFET devices. To the best of our knowledge, this performance is one of the highest performances among all furan substituted DPP based copolymers with simple OFET device geometry. In this polymer, furan flanked DPP was used as a core donor-acceptor (D-A) building block in combination with another fused aromatic electron donating dithienothiophene DTT comonomer. The combination of two aromatic fused conjugated building blocks (DPPF and DTT) in the backbone have a strong tendency to form π-π stacks with a large overlapping area that is favorable for effective charge carrier transport. In addition to that, the strong electron accepting DPP moiety with furan-DTT-furan electron donating building block assist to improve the intermolecular interactions arising from D-A inter-chain interaction whereas heteroatom contact induces a higher order molecular organization.

Results and Discussion

The polymer **PDPPF-DTT** was synthesized in a straightforward manner via Stille coupling polymerization (Scheme1) using 3,6-bis(5-bromofuran-2-yl)-2,5-bis(2-decyltetradecyl)pyrrolo[3,4-c]pyrrole-1,4(2H,5H)-dione (2) and 2,6-bis(trimethylstannyl)dithieno[3,2-b:2',3'-d]thiophene (4) in 69 % yield (see Experimental procedure as well). Compounds 2 and 4 were synthesized according to the earlier published procedure.[38, 31] In order to improve the solution processibility of **PDPPF-DTT** polymer, the long 2-decyl-1-tetradecyl branched alkyl chain was attached to the lactam nitrogen atom of DPPF building block. The low molecular weight fractions and other catalytic impurities present in **PDPPF-DTT** polymer was successfully removed by Sohxlet extraction using methanol, acetone and hexane solvents. The highest molecular weight and pure fraction of **PDPPF-DTT** was extracted by using chloroform solvent. The excess chloroform was removed by rotary evaporation and the viscous **PDPPF-DTT** polymer solution in chloroform was precipitated in excess methanol as a non-solvent. The polymer was filtered and dried under vacuum for further characterization. This purified polymer is soluble in various organic solvents such as chlorobenzene, chloroform and toluene at room temperature due to the longer branched alkyl chain. The molecular weight of purified **PDPPF-DTT** polymer was determined by high temperature gel permeation chromatography (GPC). The number average (M_n) and weight average molecular weight (M_w) are 24726 and 55035 g/mol, respectively, at a column temperature of 160 °C using trichlorobenzene as eluent. The thermal properties of **PDPPF-DTT** were evaluated by thermogravimetric analysis (TGA) and differential scanning calorimetry (DSC) techniques, respectively. TGA showed 5% weight loss decomposition temperature at 389 °C under nitrogen (See SI). Such a high decomposition temperature clearly indicates an extremely high thermal stability of the polymer. DSC heating and cooling cycles were repeated two times from room temperature till 350 °C. **PDPPF-DTT** exhibits an endothermic peak at 336 °C and an exothermic peak at 347 °C during the second heating-cooling cycles respectively (See SI). These peaks are related to the melting and crystallization temperatures of this polymer (see Supplementary Information). Additional two exothermic peaks observed at 255 °C and 229 °C and they might be arising from the longer branched alkyl side chain transitions.

The optical properties of **PDPPF-DTT** in solution and thin film were characterized by UV-vis-NIR spectroscopy as shown in Figure 1a. For the solution measurement, the polymer solution in chloroform was used whereas for the thin film, the thin layer of polymer was spin coated onto the glass slide**. PDPPF-DTT** exhibits wide UV-vis-NIR absorption starting from 350 nm to 900 nm. A strong absorption between 500 to 900 nm has been

observed for **PDPPF-DTT** polymer which is in the same range compared to the other DPP based polymers. The absorption maximum (λ_{max}) has been recorded at ~782 nm in solution. For thin film, the λ_{max} is almost identical as that of solution λ_{max} and only the difference is the broadness of peak in solid compared to solution. The solution and thin film optical absorption similarity might be attributed to the aggregation of **PDPPF-DTT** polymer in solution at room temperature even the polymer seemed to be completely dissolved. The absorption cut off for the solid UV-vis-NIR measurement is around 880 nm in solution whereas in the solid state, the cut off value measured around 905 nm. The optical band gap (E_g^{opt}) was determined from the absorption cut-off of in the solid state and which has found around 1.37 eV, demonstrating that **PDPPF-DTT** is a small band gap semiconductor. The HOMO energy level of **PDPPF-DTT** was calculated by photoelectron spectroscopy in air (PESA) method using a spin coated thin film of polymer on the glass substrate. The surface of **PPPD-DTT** polymer thin film was slowly bombarded with ultraviolet energy and then slowly polymer thin film started emitting photoelectrons of certain energy level. This energy is known as photoelectron work function. The photoelectron output is plotted with horizontal X-axis as the UV energy applied and the vertical Y-axis as the standardized photoelectron yield ratio, the result is a line with a specific slope of degree (Y/eV).

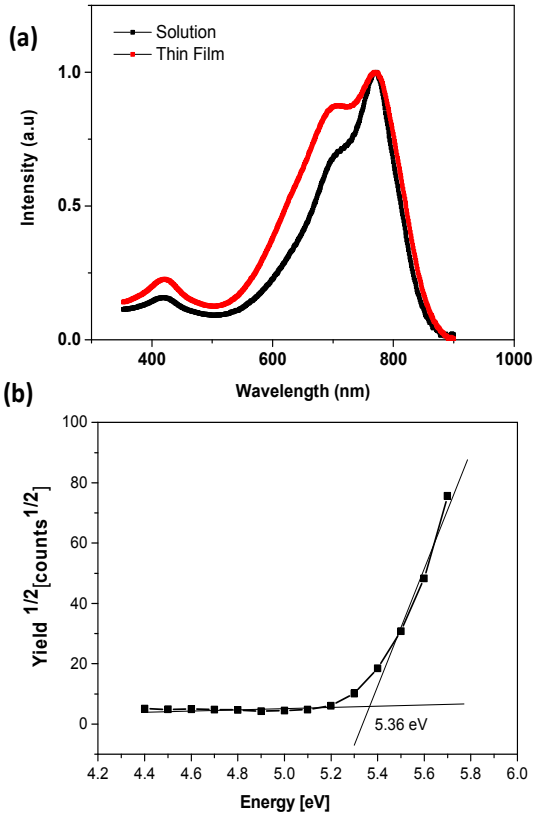

Figure 1. (a) UV-vis absorption spectra of **PDPPF-DTT** in chloroform solution and in thin film and (b) Photoelectron spectroscopy in air (PESA) analysis of **PDPPF-DTT** spin coated thin films on glass.

The HOMO value of **PDPPF-DTT** was calculated from the onset energy level recorded in PESA and which is shown in Figure 1b. The HOMO value for **PDPPF-DTT** is -5.36 eV and therefore it is expected to use this material as a good donor polymer in OFET devices. The obtained deeper HOMO is appropriate for the higher oxidation stability.

Grazing Incidence Wide Angle X-ray Scattering (GIWAXS) investigated the crystallinity and crystalline orientation within thin films of **PDPPF-DTT**. Figure 2 shows the resulting 2D scattering patterns along with the in-plane (horizontal) and out-of-plane (vertical) scattering directions. Both the as cast and annealed films display a single broad semi crystalline alkyl stacking peak at q=3.2 nm^{-1} (annealed) and q=3.6 nm^{-1} (as-cast) corresponding to an average alkyl stacking distance (from one backbone to another across the alkyl side chains) of 1.965(2) nm (annealed) and 1.73(2) nm (as-cast). The coherence length of alkyl stacking is 7.5(1) nm and 4(1) nm for annealed and as cast films, respectively. This sharpening of the scattering peaks upon annealing indicates that crystallinity increases dramatically upon annealing, producing larger and more evenly spaced stacking through the film. A second broad peak, corresponding to the π-stacking direction, is found at q=1.56 nm^{-1} (annealed) and 1.49 nm^{-1} (as cast), corresponding to 0.40 nm and 0.43 nm respectively. The coherence length of stacking in the pi direction (out-of-plane) is 1.3 nm (annealed) and 1.0 nm (as cast) indicating that this stacking is largely amorphous (only 2-3 repeat units per coherence length).

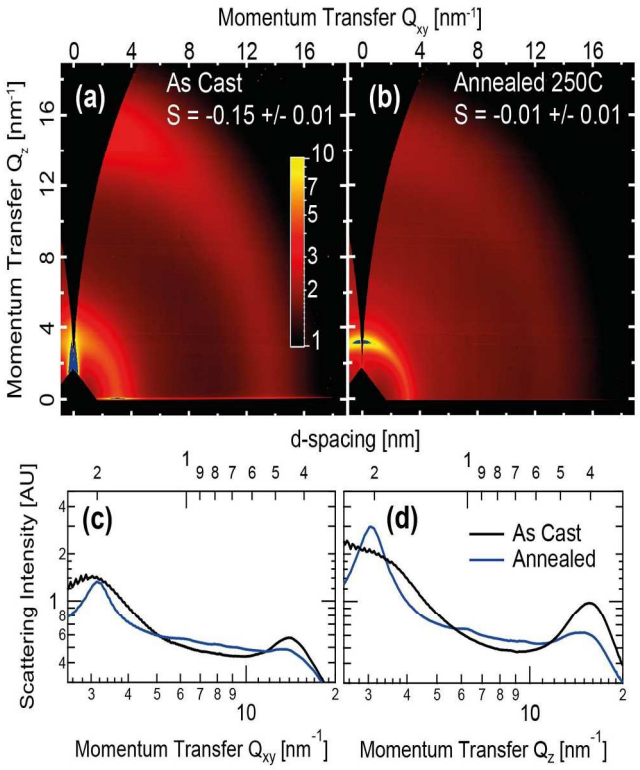

Figure 2. 2D scattering patterms of (a) as cast and (b) 250°C annealed thin films of **PDPPF-DTT**. For clarity, we also show sector plots in the (c) horizontal, in-plane direction and (d) vertical, out-of-plane direction.

Interestingly, the stacking observed for the as-cast film is largely face-on, with a herman's orientation order parameters [44] (which runs from perfectly face-on at -0.5 to perfectly edge-on at 1.0) of -0.01 +/- 0.01 for the annealed sample, indicating no preferred orientation, and -0.15 for the as-cast sample, indicating a preference for face-on packing. In order to support GIWAXS data, we also investigated conventional **XRD** measurement. **PDPPF-DTT** spin coated on Si/SiO_2 substrate and thin film annealed at 250 °C showed a strong primary peak at 4.63°, which corresponds to a d spacing of 19.1 Å as shown in Figure 3a. The observed interlayer spacing distance for **PDPPF-DTT** polymer is in the similar range with respect to earlier reported thiophene flanked diketopyrrolopyrrole with dithienothiophene (**PDTTDPP-** d-spacing of 20.3 Å**)** and selenophene flanked diketopyrrolopyrrole with dithienothiophene (**PSeDPPDTT-** d-spacing of 19.22 Å) copolymers.[38, 40] An illustrative lamellar structure of **PDPPF-DTT** in the thin film form for getting clear understanding of interlayer spacing and π-π stacking is represented (see Figure 3b). GIWAXS data is also supported with additional 2-D XRD measurements and the primary (100) and secondary (010) diffraction peaks observed from normal and parallel incident 2-D XRD measurements are attributed to interlayer spacing and π-π stacking distance respectively (see Figure 3c and 3d). During 2D XRD measurement, the diffractogram exhibits a primary diffraction peak (100) at 2θ = 4.72° (d = ~18.69 Å) when the incident X-ray is normal to the polymer flakes whereas in parallel mode, the diffraction peak (100) measured at 2θ = 4.81° (d = ~18.38 Å).

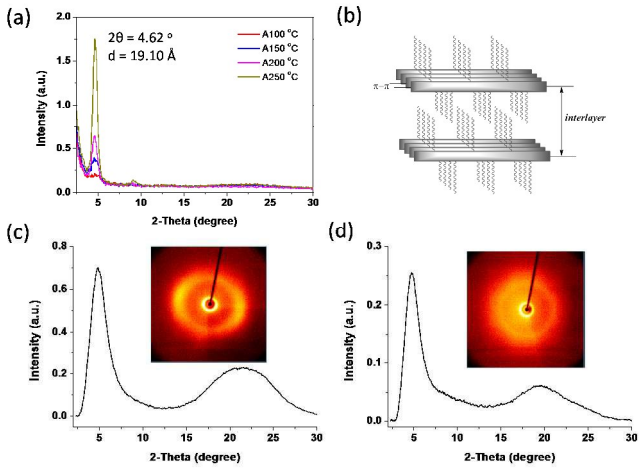

Figure 3. (a) XRD data obtained from spin-coated **PDPPF-DTT** thin films (~35 nm) on OTS modified SiO_2/Si substrates annealed at different temperatures (b) graphical lamellar structures of **PDPPF-DTT** in the thin film (c) 2-D XRD pattern intensity graphs (2-D XRD images in inset) obtained with the incident X-ray parallel and (d) perpendicular to the thin film stack **PDPPF-DTT** copolymer.

The observed interspacing values obtained from conventional wide-angle XRD measurements are in a well agreement with 2D-XRD measurements and found to be in the range of 18.38 to 19.1 Å. The broad featureless secondary diffraction peak suggests that all the polymer backbones are not aligned normal to the substrate. The broad peak from 2θ = 16.50 ° to 25.50 ° probably reflects from both the π-π stacking distance of the crystalline domains and the short range order of the amorphous region in the polymer thin films. The distance calculated from the broad peak maxima at 2θ = 19.90° and 2θ = 21.43° in normal and parallel modes are d = ~4.45 Å and d = ~4.14 Å respectively. The differences is stacking distances and limited enhancement in diffraction pattern in parallel and perpendicular conditions of **PDPPF-DTT** suggests that the polymer chain in thin films may have a mixed edge on, face on and tilted orientations. Such kind of molecular organization was also observed for other furan flanked DPP polymer **PDBFBT.**[36] Despite of mixed orientations, **PDBFBT** polymer exhibited high charge carrier mobility of 1.54 cm^2/Vs in OFET devices. [36] The electrical properties of **PDPPF-DTT** as an active channel semiconductor in OFET devices were evaluated using a bottom-gate, top-contact geometry. Heavily n-doped silicon wafer with a layer of ~200 nm SiO_2 on the surface was used as the substrate. The SiO_2 functions as the gate insulator and the doped Si as the gate. The active polymer thin film (~40 nm) was spin coated on top of an octadecyltrichlorosilane (OTS) modified SiO_2 surface using a **PDPPF-DTT** solution in chloroform (7 mg/mL) at 1000 rpm for 60 seconds. The polymer thin films were annealed at 100 °C, 150 °C, 200 °C and 250 °C respectively for 20 min on a hot plate in nitrogen atmosphere. On top of **PDPPF-DTT** thin film, gold was deposited as source and drain electrode via shadow masking method. The schematic of OFET device is shown in Figure 4a. OFET devices exhibit typical p-channel electrical characteristics (Figure 4b and 4d). The hole mobility was calculated from the saturation regime of transfer curve.

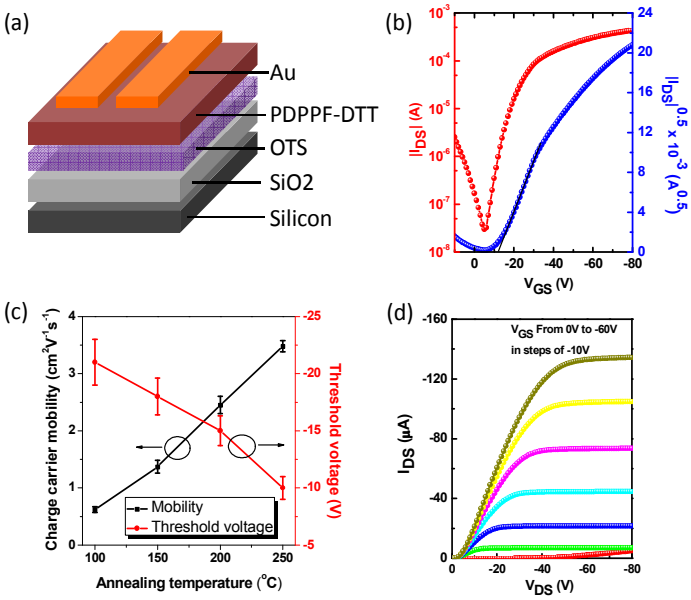

Figure. 4 (a) The schematic OFET device geometry used in this study and (b) the transfer characteristics of PDPPF-DTT OFET devices pre-annealed at 250°C. (c) Charge carrier mobilities and threshold voltage as a function of annealing temperatures. (d) The output characteristics of PDPPF-DTT OFET devices pre-annealed at 250°C. Device dimensions: channel length = 100 μm; channel width = 1 mm. All devices are measured in a dry N_2 filled glove box

Cite this: DOI: 10.1039/c0xx00000x

www.rsc.org/xxxxxx

ARTICLE TYPE

Table 1. OFET device performance of **PDPPF-DTT** thin films annealed at 100, 150, 200 and 250 °C on OTS treated n+-Si/SiO_2 substrates using bottom-gate, top-contact (BGTC) devices.

	TA	hole		
		$\mu[cm^2V^{-1}s^{-1}]$	V_T [V]	On/off
PDPPF-DTT	100	0.46-0.68	-21	10^5
PDPPF-DTT	150	1.05-1.48	-18	10^5
PDPPF-DTT	200	2.03-2.60	-15	10^5
PDPPF-DTT	250	3.18-3.56	-10	10^4

The polymer thin film annealed at 100 °C exhibited hole mobility in the range of 0.46 to 0.68 cm^2/Vs. Upon further enhancing the maximum to 1.48 cm^2/Vs. Interestingly, when the annealing temperature is further increased to 200 °C, the hole mobility was improved further up to 2.60 cm^2/Vs. The polymer annealed at 250 °C showed the highest hole mobility value of 3.56 cm^2/Vs (see Figure 4c and Table 1). The transfer and output characteristics of 250 °C annealed **PDPPF-DTT** based devices are shown in Figure 4b and 4d respectively. It should be noted that ambipolar behavior with weak electron transport could be observed due to its low band gap nature. The on/off ratio for all of the devices was around 10^5 whereas the threshold voltage observed decreased from -21 V to -10 V when increasing the annealing temperature due to reduced charge traps. According to our knowledge, the reported hole mobility of 3.56 cm^2/Vs for **PDPPF-DTT** is one of the highest hole mobility values based on the furan flanked DPP based copolymers using straightforward simple geometry. This value is also one of the highest values among dithienothiophene-based copolymers. A fused aromatic moiety such as DPP and DTT in the backbones makes this particular polymer a very planar system which enhances the orbital overlapping for better charge transport. In addition to that a conjugated alternating D−A polymer offers the feasibility of creating a ground-state partial charge-transfer state and such weakly polarized state would assist for the effective charge transport. This clearly demonstrates that prejudicially designed using easily accessible fused aromatic building block via appropriate manner can achieve such an impressive mobility. In order to study the effect of annealing temperature on the OFET performance, we also conducted morphological investigation of **PDPPF-DTT** thin film using various preannealing temperature via atomic force microscopy (AFM). The AFM images reveals the dependence of the mobility values on the morphology of the polymer thin films related to the various annealing temperature (see Figure S5 in Supporting Information). From the AFM images of the polymer thin films, it can be observed that the non-annealed polymer thin film exhibits some sort of protrusion which can resembles "stripes" on to a continuous film. Such protrusions can be arises due to the morphological inhomogeneties and they can be disappeared upon annealing. At the 250 °C annealed sample, the domain size increased to micrometer scale and covered entire film (RMS roughness = 2.21 nm). We strongly believe that an efficient charge transport in **PDPPF-DTT** semiconductor thin films annealed at 250 °C is due to interconnected network of large domains. The compact crystalline domains in the thin films with an increasing annealing temperature is in a good agreement with the XRD results, this clearly demonstrate the enhancement in crystallinity of the thin films upon annealing from lower to higher temperature. Such a highly ordered morphology is complimentary for the efficient charge transport trails between source and drain electrodes. A good planarity and the strong electron withdrawing and donating capabilities of highly fused aromatic DPP and DTT moiety enhances a strong intermolecular interaction which leads significant ordering and preferably oriented molecular organization and thus enables efficient charge transport with a high mobility in **PDPPF-DTT** polymer based OFETs. In addition to that S...S interaction and enhancement in structural planarity endorses extensive intramolecular π-conjugation and close intermolecular π-π stacking. π- Conjugated dithienothiophene-based molecules self-organize into single-crystal microribbons via attractive intermolecular S…S interactions by a simple solution process and noticeably high hole mobilities of up to 10.2 cm^2 /Vs has been achieved in organic single-crystal field-effect transistors.[45] However, by combining dithienothiophene with furan substituted diketopyrrolopyrrole can achieve such an impressive 3.56 cm^2/Vs mobility in polydipserse polymer based OFETs in comparison with monodisperse single crystal. These results clearly reveal that an appropriate fused aromatic donor-acceptor based molecular design could achieve an impressive performance in *p*-channel OFETs using elegant synthesis and modest device geometry. Such polymer can be also highly potential class of materials for fabricating logic gate devices via nanostructuration approach[46] owing to their high mobility. A significant improvement in electrical performance for p-type small molecule [47]as well as for ambipolar polymer[48] was

successfully obtained by using such a stamp-assisted deposition approach where lithographically controlled wetting and micromolding in capillaries plays a major role.

Conclusions

In summary, we have successfully designed and synthesized a new solution processable polymer semiconductor **PDPPF-DTT** by combining a furan flanked diketopyrrolopyrrole and diehtienothiophene fused aromatic building blocks via Stille coupling. **PDPPF-DTT** exhibits wide UV-vis-NIR absorption starting from 350 nm to 900 nm with a lower optical band gap of 1.37 eV. The calculated HOMO value of 5.36 eV for **PDPPF-DTT** makes it suitable candidate for stable *p*-channel OFET devices. Top contact bottom gate OFET devices based on **PDPPF-DTT** as an active channel semiconductor showed hole mobility as high as 3.56 cm^2/Vs annealed at 250 °C. The measured hole mobility value observed in **PDPPF-DTT** polymer is one of the highest values among known furan flanked DPP based organic semiconductors. Such a high mobility value and elegant synthesis opens up many possibilities to use the fused furan flanked DPP as a promising building block for synthesizing novel high performance conjugated polymers.

Acknowledgements

The authors thank the Institute of Materials Research and Engineering (IMRE), Agency for Science, Technology and Research (A*STAR) and the "Printable high performance semiconducting materials for OPVs and OTFTs" for financial support. J. W. acknowledges financial support from IMRE core funding (IMRE/13-1C0205). We are also thankful to Mr. Poh Chong Lim for his help in 2-D XRD of the polymer. PS is also thankful to the Queensland University of Technology, Brisbane and ARC for Future Fellowship Support.

Notes and references

[a]*Institute of Materials Research and Engineering (IMRE), Agency for Science, Technology, and Research (A*STAR), 3 Research Link, Singapore 117602*

[b]*Current Address: School of Chemistry, Physics and Mechanical Engineering, Queensland University of Technology (QUT), 2 George Street, Brisbane, QLD-4001, Australia, E-mail: sonar.prashant@qut.edu.au*

[c]*Department of Chemistry, National University of Singapore, 3 Science Drive 3, 117543, Singapore*

[d]*Australian Synchrotron, 800 Blackburn Road, Clayton, VIC, 3168, Australia*

[e] *Department of Materials Engineering, Monash University, Wellington Road, Clayton VIC, 3800, Australia*

†Electronic Supplementary Information (ESI) available: NMR data of starting monomers 2 and 4, DSC and TGA data of monomers and **PDPPF-DTT**. See DOI: 10.1039/b000000x/

References

1. Y. Li, P. Sonar, L. Murphy, W. Hong, *Energy Environ. Sci.,* 2013, **6**, 1684.
2. X. Guo, A. Facchetti, T. J. Marks, *Chem. Rev.* 2014, **18**, 8943.
3. A. Pron, M. Leclerc, *Prog. Polym. Sci*. 2013, **38**, 1815.
4. C. B. Nielsen, M. Turbiez, I. McCulloch, *Adv. Mater*. 2013, **25**, 1859.
5. I. Meager, M. Nikolka, B. C. Shorroeder, C. B. Nielsen, M. Planells, H. Bronstein, J. W. Rumer, D. I. James, R. S. Ahsraf, A. Sadhanala, P. Hayoz, J.C. Flores, H. Sirringhaus, I. McCulloch, *Adv. Funct. Mater*. 2014, **24**, 7109.
6. J. D. Yuen, F. Wudl, *Energ. Environ. Sci*. 2013, **6**, 391.
7. L. Biniek, B. C. Schroeder, C. B. Nielsen, I. McCulloch, *J. Mater. Chem*. 2012, **22**, 14803.
8. H. Klauk, Ed. WILEY-VCH, *Organic Electronics: Materials, Manufacturing, and Applications Weinheim*, Germany, 2006.
9. Y. Zhao, Y. Guo, Y. Liu, Y. *Adv. Mater*. 2013, **25**, 5372.
10. H. Sirringhaus, *Adv. Mater*. 2013, **26**, 1319.
11. C. Wang, H. Dong, W. Hu, Y. Liu, D. Zhu, *Chem. Rev*. 2011, **4**, 2208.
12. M. A Naik, S. Patil, *J. Polym. Sci., Part A: Polym. Chem*. 2013, **51**, 4241.
13. J. W. Wu, S. W. Cheng, Y. J. Cheng, C. S. Hsu, *Chem. Soc. Rev*. **2015**, 44, 1113.
14. A. Facchetti, *Mater. Today*, 2013, **16**, 123.
15. A. Facchetti, *Chem. Mater*. 2011, **23**, 733.
16. I. Etxebarria, J. Ajuria, R. Pacios, *Org. Elect*. 2015, **19***,* 34.
17. I. L. Kang, H.J. Yun, D. S. Chung, S. K. Kwon, Y. H. Kim, *J. Am. Chem. Soc.*, 2013, **135**, 14896.
18. G. Kim, S. J. Kang, G. K. Dutta, Y. K. Han, T. J. Shin, Y. Y. Noh, C. Yang, *J. Am. Chem. Soc.*, 2014, **136**, 9477.
19. H. Zhou, L. Yang, S.C. Price, K. J. Knight, W. You, *Angew. Chem. Int. Ed*., 2010, **122**, 8164.
20. M. Zhang, Y. Gu, X. Guo, F. Liu, S. Zhang, L. Huo, T. P. Rusell, J. Hou, *Adv. Mater.*, 2013, **25**, 4944.
21. Y. Yamashita, *Chem. Lett.* 2009, **38**, 870.
22. R. Po, G.Bianchi, C. Carbonera, A. Pellegrino, *Macromolecules*, 2015, **48**, 453.
23. H. Sirringhaus, M. Bird, T. Richards and N. Zhao, *Adv. Mater.*, 2010, **22**, 3893
24. P. Deng, Q. Zhang, *Polym. Chem*., 2014, **5**, 3298.
25. C. M. Chen, S. Sharma, Y. L. Li, J. J. Lee, S. A. Chen, J. *Mater. Chem. C*, 2015, **3**, 33
26. I. Osaka, M. Akita, T. Koganezawa, K. Takimiya, *Chem. Mater*., 2012, **24**, 1235.
27. M. Grzybowski, D. T. Gryko, *Adv. Opt. Mater*. 2015, **3**, 280.
28. B. Sun, W. Hong, Z. Yan, H. Aziz, Y. Li, *Adv. Mater*. 2014, **26**, 2636.
29. P. Sonar, T. R. B. Foong, S. P. Singh, Y. Li, A. Dodabalapur, *Chem. Commun*. 2012, **48**, 8383.
30. P. Sonar, S. P. Singh, E. L. Williams, Y. Li, M. S. Soh, A. Dodabalapur, *J. Mater. Chem.,* 2012, **22**, 4425.
31. P. Sonar, T. J. Ha, Y. Seong, S. C Yeh, C. T Chen, S. Manzhos, A Dodabalapur, *Macromol. Chem. & Phys*. 2014, **215**, 725.
32. Y. Li, P. Sonar, S. P. Singh, Z. E. Ooi, E. S. H. Lek, M. Q. Y. Loh, *Phys. Chem. Chem. Phys*. 2012, **14** , 7162.
33. P. Sonar, J. M. Zhuo, L. H. Zhao, K. M. Lim, J. Chen, A. J. Rondinone, S.P. Singh, *J. Mater. Chem.*, 2014, **22**, 17284.
34. P. Sonar, T. J Ha, A Dodabalapur, *Chem. Comm*., 2013, **49**, 1588.
35. H. Chen, Y. Guo, Z. Mao, D. Gao, G. Yu, *J. Poly. Sci., Part-A: Poly. Chem*. 2014, **52**, 1970.
36. Y. Li, P. Sonar, S. P. Singh, W. Zeng, M. S. Soh, *J. Mater. Chem*., 2011, **21**, 10829.
37. T. J. Ha, P. Sonar, A Dodabalapur, *ACS Appl Mater. & InterfAces*, 2014, **6**, 3170.
38. J. W. Jung, F. Liu, T. P. Russell, W. H. Jo, *Energy Environ. Sci*., 2012, **5**, 6857.

39. J. Li, H. S.Tan Z.K Chen, W. P. Goh, H. K. Wong, K. H. Ong, W. Liu, C. M. Li, B. S. Ong, *Macromolecules*, 2011, **44** , 690.
40. M. Shahid, R. S. Ashraf, Z. Huang, A. J. Kronemeijer, T. M. Ward, I. McCulloch, J. R. Durrant, H. Sirringhaus, M. Heeney, *J. Mater. Chem*., 2012, **22**, 12817.
41. J. Youn, P. Y, Huang, S. Zhang, C. W. Liu, S. Vegiraju, K. Prabhakaran, C. Stern, C. Kim, M. C. Wu, C. C. Liu, C. Kim, H. C. Lin, M. C. Chen, A. Facchetti, T. J. Marks, *J. Mater. Chem. C* 2014, **2**, 7599.
42. S. S. Cheng, P. Y. Huang, M. Ramesh, H. C. Chang, L. M. Chen, C. M. Fung, M. C. Wu, C. C. Liu, C. Kim, H. C. Lin, M. C. Chen, C. W. Chu, *Adv. Funct. Mater*. 2014, **24**, 2057.
43. J. Youn, M. C. Chen, Y. J. Liang, H. Huang, R. P. Ortiz, C. Kim, C. Stern, T. S. Hu, L. H. Chen, J. Y. Yan, A. Facchetti, T. J. Marks, *Chem. Mater*. 2010, **22**, 5031.
44. L. A. Perez, P. Zalar, L. Ying, K. Schmidt, M. F. Toney, T. Q. Nguyen, G. C. Bazan, E. J. Kramer, *Macromolecules*, 2014, **47**, 1403.
45. Y. S. Tang, T. Yasuda, H. Kaizoe, H. Mieno, H. Kinko, Y. Tateyama, C. Adachi, *Chem. Commun*. 2013, **49**, 6483.
46. D. Gentili, F. Valle, C. Albonetti, F. Liscio, M. Cavallini, *Acc. Chem. Res.*, 2014, **47**, 2692.
47. M. Cavallini, P. Stoliar, Jean-F. Moulin, M. Surin, P. Leclère, R. Lazzaroni, D. W. Breiby, J. W. Andreasen, M. M Nielsen, P. Sonar, A. C Grimsdale, K. Müllen, F. Biscarini *Nano Lett.*, 2005, **5**, 2422.
48. D. Gentili, P. Sonar, F. Liscio, T. Cramer, L. Ferlauto, F. Leonardi, S. Milita, A. Dodabalapur, M. Cavallini *Nano Lett.*, 2013, **8**, 3643.